



Spectral characteristics and morphology of nanostructured Pb–S–O thin films synthesized via two different methods



H.S.H. Mohamed^{a,b,*}, M. Abdel-Hafiez^{a,c}, B.N. Miroshnikov^b,
A.D. Barinov^b, I.N. Miroshnikova^b

^a Faculty of Science, Fayoum University, 63514 Fayoum, Egypt

^b National Research University, MPEI, Krasnokazarmennaya 14, Moscow 111250, Russian Federation

^c Center for High Pressure Science and Technology Advanced Research, 1690 Cailun Rd., Shanghai, 201203, China

ARTICLE INFO

Keywords:

Spectral characteristics
PbS thin films
Morphology
Chemical vapor deposition
Physical vapor deposition

ABSTRACT

Using two different experimental techniques, namely chemical vapor deposition (CVD) and physical vapor deposition (PVD), we deposited a lead sulphide (PbS) thin films with a very small lifetime (10^{-9}). We investigated the morphology of the obtained PbS films using various techniques i.e. AFM, SEM, EDAX, AES and HRTEM. In the case of CVD, we found that the surface consists of grains with dimensions in the plane (diameter to 300 nm and height up to 200 nm), while the same order of the grain size has been observed for PVD. On the other hand, SEM investigation reveals that the PbS particles with various morphologies of both films have uniform and the particle size distribution. Small amount of sodium was obtained from EDXS studies, which may originate from the substrate where the deposition process has been produced at temperature 550–600 °C and for CVD at minimum accelerating voltage 5 kV silicon are presented in the spectrum, which means that the region for X-ray generation voltage data exceeds the thickness of the films (where the thickness of films about 0.4 μm). AES confirms the surface layer of these films (PVD) containing carbon and oxygen and it has a thickness of 0.1 μm . At a depth of 1.3 μm in films these elements are again increased, which corresponds to the film thickness of 1.5 μm . Layers of PVD films are seen by HRTEM and the studies confirm that oxygen-layer located on top of the structure, while the layers of CVD films not only have the oxygen along the crystallite boundaries, but also accumulate in the depth of the boundary with the substrate. Our results of morphology indicate that the change in spectral characteristics of films deposited by (CVD and PVD) is related to the structure and the crystalline size.

© 2014 Elsevier Ltd. All rights reserved.

1. Introduction

Solar cell technologies are becoming increasingly important in electric power generation. This is due to the fact that they provide more secure power sources and pollution free electric supplies. Semiconductor thin films

are always in focus due to their outstanding electronic and optical properties and possible applications in various devices such as light-emitting diodes [1–4], single electron transistors and field effect transistors [12]. The fabrication of nanocrystalline semiconducting metal chalcogenide has drawn considerable interest in recent years, because of their unusual optical and electric properties and potential applications in nanodevices [6–8]. In recent years, numerous efforts have been made to control the fabrication of nanostructured materials with various morphologies,

* Corresponding author.

E-mail address: hsh02@fayoum.edu.eg (H.S.H. Mohamed).

since the novel properties and potential applications of nanomaterials depend largely on their shapes and sizes [9–11]. The electronic and optical properties of semiconductor materials can be changed by changing their size and shapes [13] as an important IV–VI group semiconductor. PbS is an important direct narrow band gap semiconductor material (≈ 0.41 eV) with a large excitation Bohr radius of 18 nm [14–17]. Furthermore, it has been widely used in many fields such as Pb^{2+} ion-selective sensors [18], IR detector [19], photography [20,21], and solar cell absorption [22–24]. Additionally, due to the non-linear optical properties of the PbS, it presents various applications in optical devices i.e., optical switch [25]. PbS has been utilized as photo resistance, diode lasers, humidity and temperature sensors, decorative and solar control coatings [26,27]. For these applications, we believe that further studies in order to explore the morphology of the PbS films with different particle sizes are required. It has been reported that the particle diameters should vary from a few micrometers for infrared detector applications to several nanometers for quantum dots [28]. However, still intensive research interest in lead chalcogenides and various articles have been reported to explore new parameters in that system [30,29]. Theoretical consideration has been reported by Neustroeva and Osipova in order to further understand the structures of PbS [31,32]. Further properties of PbS layers on a silicon substrate with a sub-layer of SiO_2 have been studied [33]. Although various studies show much attention to the structure, complexity, ambiguity, and manufacture [34], but still lack information from the physics point of view in these systems.

In the respect, this work aims to explain that particular point and more information will be presented. One of the main motivations is to study the photosensitive films made from "Sapphire" because of its distinctive feature which indicated that the films made by the two methods (CVD and PVD). We demonstrate the change in spectral characteristics of films, explain the effect of oxygen on the electronic structure of the energy bands and the morphology of nanostructured films Pb–S–O.

2. Experimental

Photosensitive films from PbS were synthesized by two different methods. First of all, physical method in this method it has been used metal spraying of PbS coating in a vacuum onto heated glass substrates and subsequent heating these films to 550–600 °C at atmospheric air pressure (PVD). Second method is "chemical" methods in this method it has been used PbS layer that has been precipitated from solutions is not subjected to heating above 100–120 °C, but an additional "oxidizing agent," frequently hydrate hydrazine, is added to the solutions (CVD) [35].

The morphology and the crystallography of the Pb–S–O polycrystalline thin films were studied by atomic force microscopy, scanning the surface and energy dispersive microanalysis (EDXS) and high resolution transmission electron microscopy (HRTEM).

3. Results and discussion

3.1. Spectral characteristics of Pb–S–O

The spectral characteristics of both PVD and CVD films have been investigated in [36–38]. In the case of PVD (annealing process followed by heating) the spectral characteristics have a peak near the wavelength, (λ) = 2.5 μm and, corresponding to the bandgap (E_g = 0.4 eV at room temperature) as shown in (Fig. 1 lower panel). While for CVD films the spectral characteristics have several maximum, which are similar to the structures of the sandwich with different E_g at different (λ) as shown in (Fig. 1 upper panel). From our morphological studies we can outline the difference between them, which may originate, first of all, from the non-optimal film thickness. The thickness of CVD films is about 0.4 μm , which is different from the preferred thickness of 1.5 μm but the thickness of PVD films is about 1.5 μm . Secondly, the differences are due to the dissolving of oxygen inside the structure of PbS. It is necessary for dissolving oxygen in all sources, which will be joined with sensitive layers, bonded with electrons and increase the life time of holes where the sensitization process by heat treatment in oxygen atmosphere was used in order to increase the photoconductivity of vacuum evaporated PbS thin films [39]. These holes are represented the majority carriers. However, it should be noted that the effect of oxygen on the electronic structure of the energy bands brings, in particular, a large decrease in the energy band gap under certain conditions.

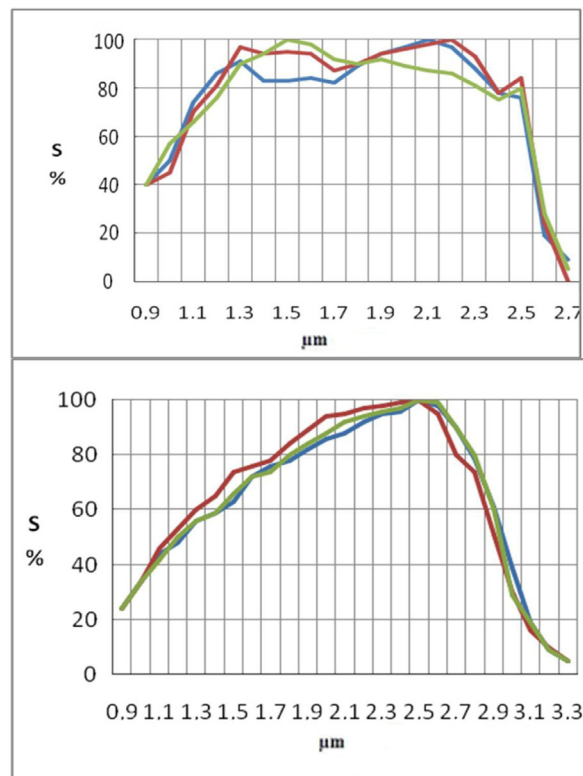


Fig. 1. Spectral characteristics of photosensitive PbS films. (upper panel) Films prepared by CVD and (lower panel) films prepared by PVD.

Oxygen is an isoelectronic impurity, which replaces chalcogen in the lattice [40]. For such substitutional impurities, which introduce appreciable local distortions into the lattice, implies a strong interaction between the localized impurity states and extended states in the conduction band. As a result of presences oxygen in PbS, even a small amount of an isoelectronic impurity gives rise to a splitting of the conduction band into two noncrossing subbands [41]. One of these subbands is formed of highly localized impurity states E_+ , while the second subband is formed of extended conduction-band states E_- that experience the effect of the narrow resonance band introduced by the isoelectronic impurity. In the literature, the localized state is positioned at 0.15 eV from trapping levels and at 0.23 eV from the recombination levels. So far,

up to date, still lack of information which explain the reduction of energy gap by Urbach and the last years the role of oxygen in the structures of photosensitive materials, etc quite ambiguous where the oxygen defect plays an important role in the sensitive layers [42]. One can understand from the latter point that our spectral characteristics of the energy scale would be expected in case of (CVD) and we expect the possibility of appearance effect Moss Burstein, which has been known in the structures based on InSb.

3.2. Morphological and structure composition obtained for Pb–S–O films

PbS have attracted much attention in recent years due to their interesting morphology and potential applications

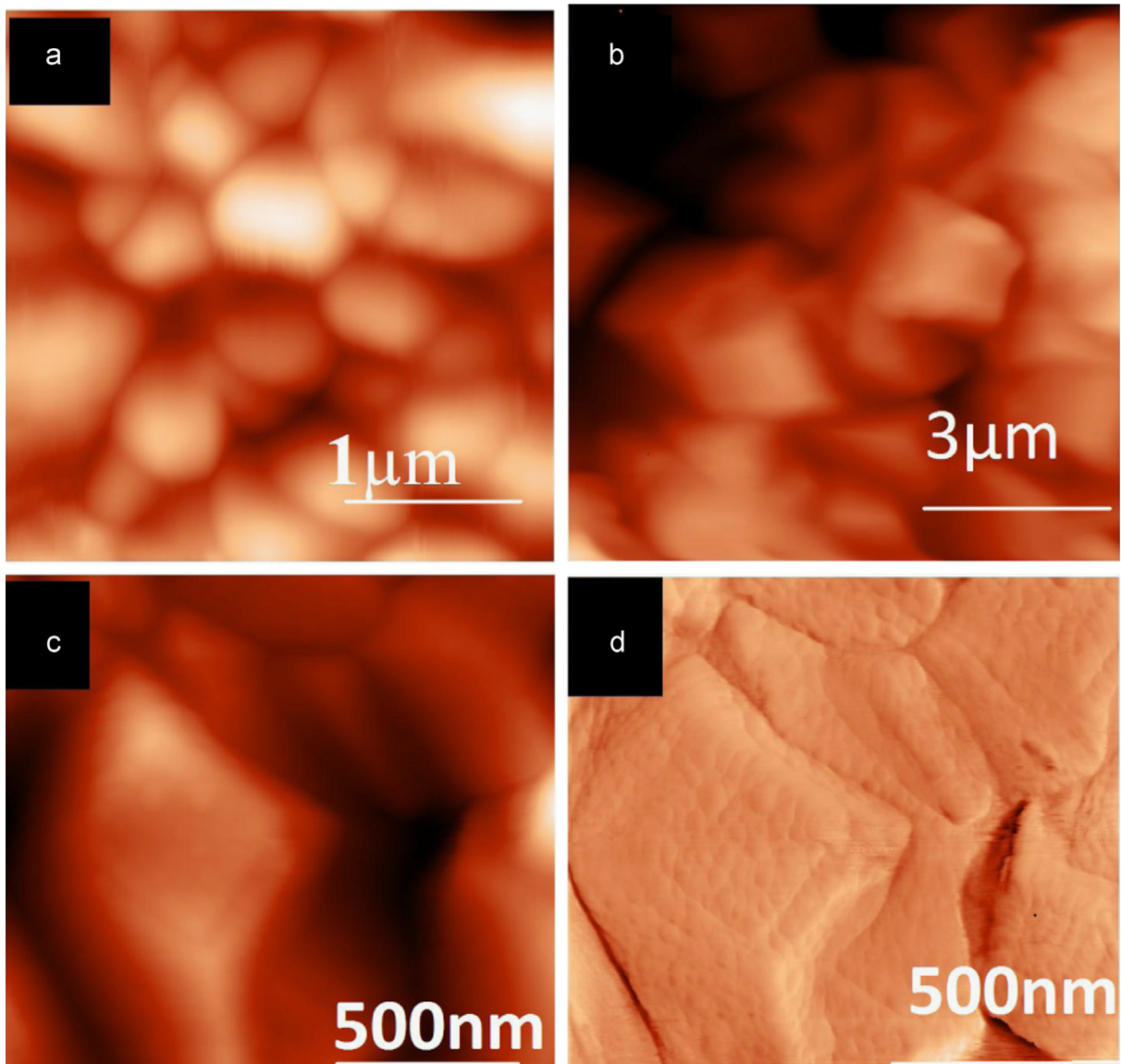


Fig. 2. AFM picture of photosensitive PbS films. (a) corresponds to scan the surface of the photosensitive layer produced by CVD, (b) corresponds to scan the surface of the photosensitive layer produced by PVD, (c) scan the PVD films in nanoscale to obtain the small grains in each cubic and (d) signal LF for PVD.

[6]. Spherical shapes of the CVD films revealed by AFM (Fig. 2a). It consists of small grains with dimensions in the plane of the films (diameter to 300 nm and height up to 200 nm). The surface layers of the PVD films have a nearly parallelogram (pyramid) shapes as in Fig. 2b each cube (parallelogram) consists of grains. These grains with dimensions are similar to those obtained for the CVD layer with the maximum sizes of grains are (500 nm) as in Fig. 2c. In order to observe these grains, we must also watch the signal LF (Lateral Force, change the torsion of the cantilever deflection), which emphasizes the features of relief as in Fig. 2d. The average diameter of this grain is ranging from 40 to 60 nm, while the height of grain is 3–5 nm. The morphology of physical layers has distinct crystallographic faces and correct form, which may be due to the high-temperature annealing 550–600 °C in an uncontrolled atmosphere. The main disadvantage of this method is that the measurements are a shallow depth of field compared with the SEM. Based on these results, it is hardly difficult to say whether the grains in the relief are pyramid or parallelepiped. Therefore, our results cannot talk about the real shape of grains, but it has magnitude in order of 10 nm in the surface. The SEM investigation reveals that the PbS particles with various morphologies of both films have uniform and the particle size distribution. For PVD, the films have polycrystalline form with grain sizes average of 500 nm and 600 nm, which are in line with our results obtained from the AFM as shown in Fig. 3b. For CVD films, this method does not allow us to evaluate the smoothness of the surface, which must normally influence the spectral characteristics of photoresistor as shown in Fig. 3a.

In the next step we detail the determination of chemical composition of the photosensitive layers by energy dispersive microanalysis (EDXS), which provides the change in the depth of analyzed region of the layer. Typical spectra

EDXS for samples prepared by “PVD” and “CVD” are shown in Fig. 4 and Table 1. EDXS studies reveals that films deposited by PVD existence of small amount of sodium is about 0.4–1.6 wt% (see Fig. 4b) in the entire thickness of the film when accelerating voltage of electron beam from 5 kV to 30 kV (which the voltage of the beam determines the size of the “pear” in the region of X-ray emission). Existing of sodium may be due to its diffusion from the substrate into the film, where the deposition process has been produced at temperature 550–600 °C [43]. We accelerate voltage from 15 kV to 30 kV, taking into account necessary values voltage for more accurate to determine the concentration of lead, which $L_{\alpha} \approx 10.5$ keV. Also, throughout the film shows the presence of oxygen (20–25 wt%). Carbon present in the spectrum corresponds to the physical PbS hydrocarbon contamination unless the concentration of carbon not get involved in process technology layers, but the majority of carbon contamination became after the preparing process.

For films deposited by CVD in this process should be noted that even with a minimum accelerating voltage of 5 kV present of silicon in the spectrum (see Fig. 4a), which means that the region for X-ray generation voltage data exceeds the thickness of the films (0.4 μm). It is important to note that silicone, which is observed here comes from the substrate quartz (SiO₂), and concentration ratio between silicon and oxygen is about 1:2 as we noted at $U > 20$ kV silicon concentration is constant ≈ 10.5 wt%, and at $U < 10$ kV ≈ 5 wt%, where $U > 20$ kV X-ray radiation is generated mainly from the substrate, while $U < 10$ kV – from film. It is clearly that the existence of oxygen in our films is not only from the used substrate but also has been added to preparing processes. Thus, the average concentration of oxygen in samples prepared by CVD is three times smaller than in prepared by PVD. Although it was unexpected, we had expected approximately

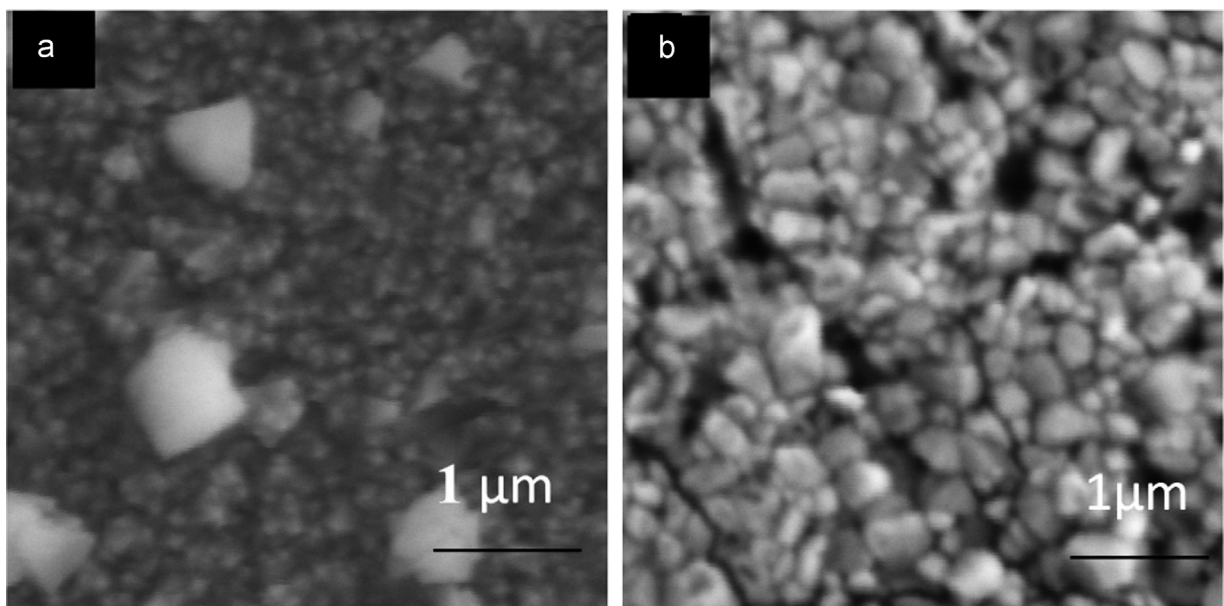


Fig. 3. SEM picture of photosensitive PbS films. (a) Films prepared by CVD and (b) films prepared by PVD.

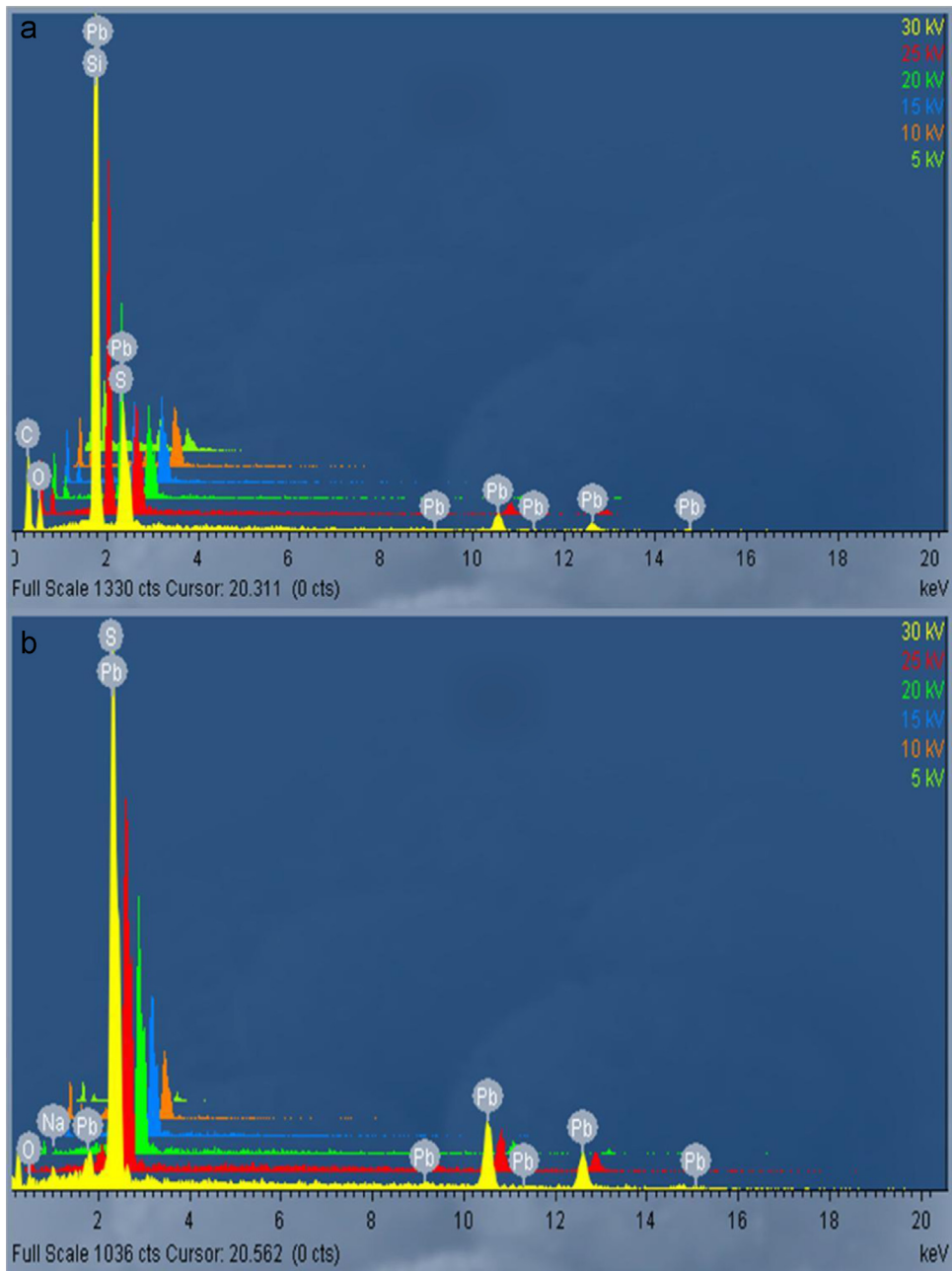


Fig. 4. EDXS spectra of photosensitive PbS films. (a) Films prepared by CVD and (b) films prepared by PVD.

Table 1

Parameters and EDAX analysis for all elements of both investigated CVD and PVD films.

Method	Thickness (μm)	R_T ($\text{M}\Omega$)	E_g (eV)	V (kV) ^a	C (wt%)	O (wt%)	Na/Si (wt%)	S (wt%)	Pb (wt%)
CVD	0.5	0.34	0.41	30	69.83	17.83	10.43	0.97	0.85
PVD	1.5	2.27	0.37	30	76.34	8.56	1.12	7.03	6.85

^a We have used various accelerating voltage ranging between 5 and 30 kV, but in this table we show only the 30 kV for comparison.

equal value [44]. Therefore, the quantitative results are not conflicting with the data on the morphology, but it cannot provide dependable information on the distribution

of oxygen in the photosensitive layers. For the sake of comparison, we have summarized the parameters of both investigated films extracted from EDAX analysis, see Table 1.

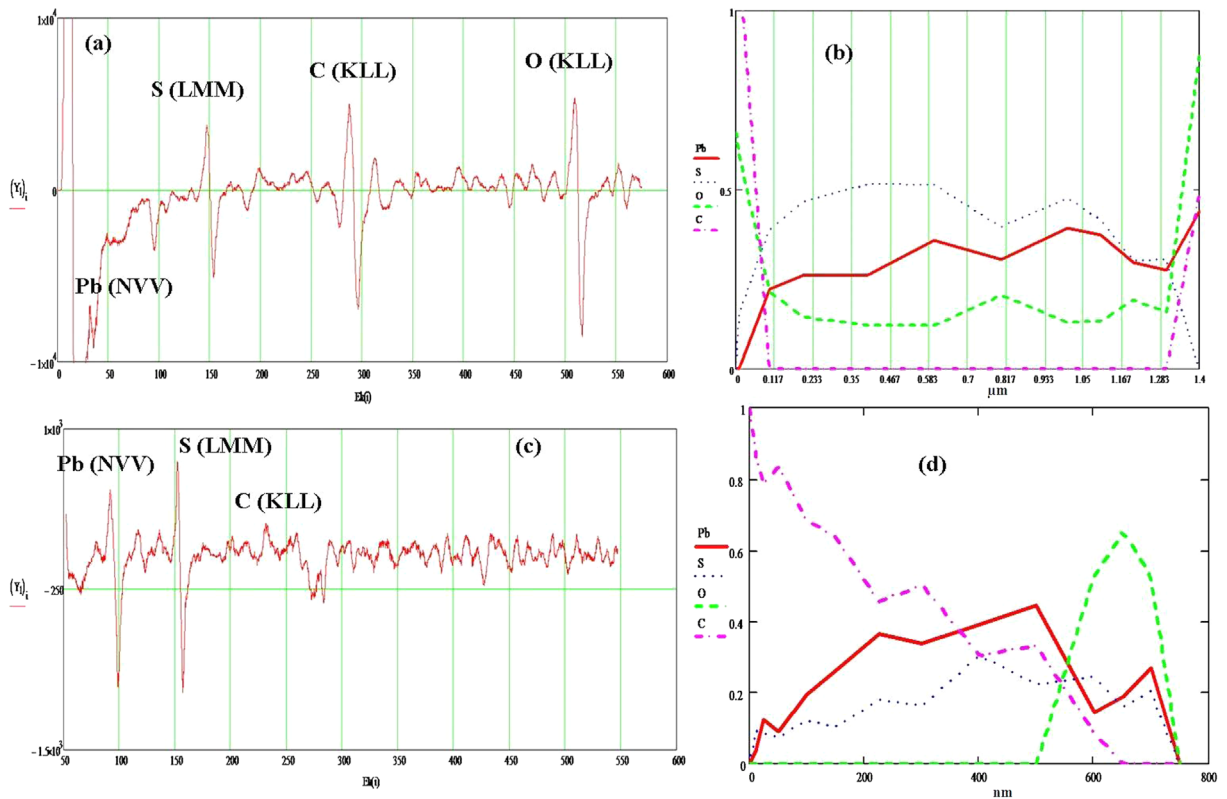


Fig. 5. AES spectra of photosensitive PbS films. (a) corresponds to Auger spectrum from samples produced by PVD, (b) shows the ratio of elemental structure to depth of samples prepared by PVD, (c) corresponds to Auger spectrum from samples produced by CVD, and (d) shows the ratio of elemental structure to depth of samples prepared by CVD.

However, from the investigated results, it is difficult to determine in which form/areas that oxygen can be positioned, we further used an Auger electron spectroscopy on LHS-10 (Leubold-Heraus, Germany) by using of coating argon layer. Fig. 5a presents the differential Auger electron spectrum of “PVD” films. Auger peak shows that Pb (NVV) has an energy of 96 eV, S(LMM) – 151 eV, C (KLL) – 275 eV and oxygen O (KLL) – 520 eV. The intensities of Auger peaks were standardized according to empirical sensitivity coefficients of corresponding Auger transitions. One clearly sees that the surface layer of these films (PVD) are containing carbon and oxygen with thickness of about 0.1 μm . We should also mention that around 1.3 μm depth in these films these elements are also increased, which corresponds to the film thickness of 1.5 μm . In Fig. 5b illustrates that at a depth of 0.8 and 1.2 μm , the oxygen ratio is significantly increasing. This fact indicates that the films mainly consist of two grain chains of crystallites on the boundary which are inclusion oxygen.

On the other hand, the oxygen ratio in CVD films is found to be less than that in PVD films. Fig. 5d shows the depth distribution of the detected elements and the thickness of these films has large carbon ratio. It is also necessary to note that this ratio is much smaller than that in PVD films. Depletion surface of the investigated films with sulfur is heated in the atmospheres, where the sulfur flies away from the surface, while at the substrate it is dissolved in the glass. The annealing process in high

temperature leads to oxide a greater portion of the film, the oxide layer is formed at the edges of the crystallites which is accumulated between them. The distribution of oxygen in CVD films is localized at 200 nm from the substrate, which means that it is formed before depositing layer of PbS, which might be due to the compound $\text{Pb}(\text{OH})_2$. Furthermore, the oxygen in CVD films substantially less than that in PVD (see Fig. 5c).

Note that the distribution of carbon in the thickness of the films is chemically deposited, with the growth of films by chemical deposition reaction mixture depleted in sulfur ions, increases the possibility of reactions with the formation of lead cyanide PbCN_2 and lead acetate $2\text{PbO} \cdot \text{Pb}(\text{CH}_3\text{COO})_2 \cdot \text{H}_2\text{O}$.

In order to further explore the crystallographic investigations, we have used HRTEM. From these studies we noticed that both PVD and CVD films have bright colors in the pictures belong to the light elements (primarily oxygen) and a dark color reflects the atoms with higher numbers (sulfur, lead). Clearly from Fig. 6 (lower panel) we see the layering structure of the PVD films, where oxygen-layer is located on top of the structure and at the edges of large crystallites. On the other hand, for the CVD films (upper panel Fig. 6), the oxygen is not only exists along the crystallite boundaries, but also accumulates in a depth on the boundary with the substrate. Thus, we can conclude that the thickness of films depends on the preparation technology and can determine a factor for the

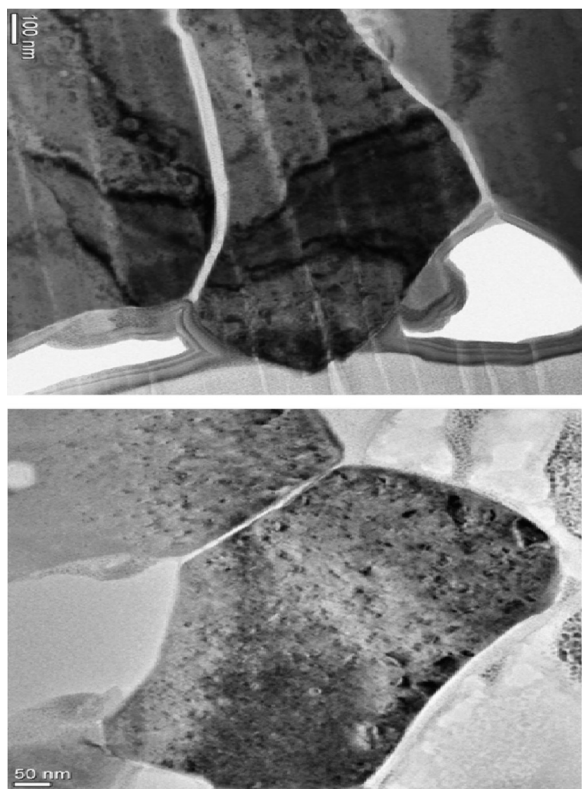


Fig. 6. TEMHR picture of photosensitive PbS films. (upper panel) Films prepared by CVD and (lower panel) films prepared by PVD.

resistance value of the layers (which varies from tens of $K\Omega$ to several $M\Omega$). So, in order to improve any devices based on the PbS polycrystalline films, the difference in surface properties and sizes should be taken into account [45].

4. Summary

In summary, we have used PVD and CVD to perform the PbS films. The investigations of morphological and spectra characteristic of PbS particles are presented. The elemental analysis of the obtained PbS particles was investigated by EDAX techniques. The fingerprint results of the PbS particles, prepared by both CVD and PVD, showed that both samples possess a cubic crystal structure, and considerable amount of oxygen in the films, but they do not have the same value. The ratio of oxygen on the metal-to-sulfur can change the spectral characteristics of PbS, the conductivity of the samples and energy gap, where oxygen can separate the conduction band into two sub-bands. Our results of morphology indicate that the change in spectral characteristics of films deposited by (CVD and PVD) is related to the structure and the crystalline size.

Acknowledgments

This work is supported by the Egyptian-Russian governments (Grant No. 12-07-00706A) and the authors

would like to thank the anonymous referee for his carefully reading the manuscript and for his valuable comments and suggestions.

References

- [1] V.L. Colvin, M.C. Schlamp, A.P. Alivisatos, *Nature* 370 (1994) 354.
- [2] Fatemeh Davar, Mohammad Reza Loghman-Estarki, Rouhollah Ashiri, *J. Ind. Eng. Chem.* 2014, <http://dx.doi.org/10.1016/j.jiec.2014.05.002> (in press).
- [3] Masoud. Salavati-Niasari, Mohammad Reza Loghman-Estarki, Fatemeh Davar, *J. Inorg. Chim. Acta* 362 (2009) 3677–3683.
- [4] K. Sankarasubramaniana, P. Soundarrajana. *Mater. Sci. Semiconduct. Process.* 26 (2014) 346–353.
- [6] Fatemeh Davar, Mohammad Reza Loghman-Estarki, Rouhollah Ashiri, *Int. J. Appl. Ceram. Technol.* 11 (4) (2014) 637–644.
- [7] Maryam Mohammadikish, Fatemeh Davar, Mohammad Reza Loghman-Estarki, *J. Clust. Sci.* 24 (2013) 217–231.
- [8] Masoud Salavati-Niasari, Mohammad Reza Loghman-Estarki, Fatemeh Davar, *J. Alloys Compd.* 475 (2009) 782–788.
- [9] Maryam. Mohammadikish, Fatemeh Davar, Mohammad Reza Loghman-Estarki, Zohreh Hamidia, *J. Ceram. Int.* 39 (2013) 3173–3181.
- [10] Masoud Salavati-Niasari, Fatemeh Davar, Mohammad Reza Loghman-Estarki, *J. Alloys Compd.* 481 (2009) 776–780.
- [11] Z. Shen, G. Chen, Q. Wang, Y. Yu, C. Zhou, Y. Wang, *J. Nanoscale* 4 (2012) 2010–2017.
- [12] B.A. Ridley, B. Nivi, J.M. Jacobsn, *Science* 286 (1999) 746.
- [13] P.D. Yang, C.M. Lieber, *Science* 273 (1996) 1836.
- [14] S. Seghaier, N. Kamoun, R. Brini, A.B. Amara, *Mater. Chem. Phys.* 97 (2006) 71.
- [15] S.B. Pawara, J.S. Shaikhb, R.S. Devanc, Y.R. Mac, D. Haranathd, P.N. Bhosalea, P.S. Patil. *Appl. Surf. Sci.* 258 (2011) 1869–1875.
- [16] S.M. Lee, Y.W. Jun, S.N. Cho, J. Cheon, *J. Am. Chem. Soc.* 124 (2002) 11244.
- [17] Fatemeh Davara, Maryam Mohammadikish, Mohammad Reza Loghman-Estark, Majid Masteri-Farahani, *Ceram. Int.* 40 (2014) 8143–8148.
- [18] H. Hirata, K. Higashiyama, *Bull. Chem. Soc. Jpn.* 44 (1971) 2420.
- [19] P. Gadenne, Y. Yagil, *J. Appl. Phys.* 66 (1989) 3019.
- [20] P.K. Nair, O. Gomezdaza, M.T.S. Nair, *Adv. Mater. Opt. Electron.* 1 (1992) 139.
- [21] Masoud Salavati-Niasari, Davood Ghanbari, Mohammad Reza Loghman-Estarki, *J. Polyhedron* 35 (2012) 149–153.
- [22] W. Chena, L. Pana, L. Chenb, Zhe Yua, Qiong Wanga, *Appl. Surf. Sci.* 309 (2014) 38–45, <http://dx.doi.org/10.1016/j.apsusc.2014.04.152>.
- [23] T.K. Chaudhari, S. Chatterjes, in: *Proceedings of International Conference on Thermo electronics*, vol. 11, 1992, p. 40.
- [24] S.K.R. Yadanaparthi, D. Graybill, R. vonWandruszka, *J. Hazard. Mater.* 171 (2009) 115.
- [25] R.S. Kane, R.E. Cohen, R. Silbey, *J. Phys. Chem.* 100 (1996) 7928.
- [26] P.K. Nair, V.M. Garcia, A.B. Hernandez, M.T.S. Nair, *J. Phys. D: Appl. Phys.* 24 (1991) 1466.
- [27] Pop, C. Nascu, V. Ionescu, E. Indrea, I. Bratu, *J. Thin Solid Films* 307 (1997) 240.
- [28] R.A. Smith, F.E. Jones, R.P. Chasmar, *The Detection and Measurement of Infrared Radiation*, Clarendon, Oxford, 1958.
- [29] Masoud Salavati-Niasari, Mohammad Reza Loghman-Estarki, Fatemeh Davar, *Chem. Eng. J.* 145 (2008) 346–350.
- [30] D.E. Aspnes, M. Cardona, *J. Phys. Rev.* 173 (1968) 714–728.
- [31] R.J. Cashman, in: *Proceedings of the National Electronics Conference*, vol. 2, 1946, p. 171.
- [32] R. J. Cashman, in: *Proceedings of the IRE* 47.9, 1959, 1471–1475.
- [33] V. Pentia, E. Goldenblum, A. Buda, M. Iordache, G. Botila, *Rom. J. Inf. Sci. Technol.* 10 (1) (2007) 53–66.
- [34] H. Elabd, A. Steckl, *J. Appl. Phys.* 51 (1980) 726.
- [35] L.N. Kurbatov, in: *Proceedings of the International Conference "Orion" Moscow*, 1996, 3–12.
- [36] L.N. Neustroev, V.V. Osipov, *Soviet Microelectronics* 17.5 (1988) 220–235.
- [37] O.A. Gudayev, V.A. Treschihin, *Optoelectronics* 5 (1992) 19–22.
- [38] T.N. Johnson, *Proc. SPIE* 443 (1984) 60.
- [39] E. Indrea, Adriana Barbu, *Appl. Surf. Sci.* 106 (1996) 498–501.
- [40] W. Shan, W. Walukiewicz, J.W. Ager, et al., *Phys. Rev. Lett.* 82 (1999) 1221.
- [41] N.K. Morozova, I.A. Karetnikov, et al., *Semiconductors* 39 (5) (2005) 485–492.

- [42] Jinping Wang, Zheng Yan, Lili Liu, Yingyi Zhang, Zuotai Zhang, Xidong Wang, *Appl. Surf. Sci.* 309 (2014) 1–10.
- [43] I.N.Miroshnikov, H.S.H. Mohammed, E.V. Zenovaetc, International Conference 2011, MPEI, Moscow, 2012, 140–145.
- [44] I.N. Miroshnikova, N.D.Vasilyeva, B.N. Miroshnikov, in: International Conference, MPEI, Moscow, 2009, 148–150.
- [45] I.N. Miroshnikov, E.A. Kalm, H.S. Mohammed, et al., in: Conference MPEI, 2011, 173–179.